2D flexural backstripping of extensional basins: the need for a sideways glance

Alan M. Roberts[1], Nick J. Kusznir[2], Graham Yielding[1] and Peter Styles[2]
[1]*Badley Earth Sciences Ltd, North Beck House, North Beck Lane, Hundleby, Spilsby, Lincs, PE23 5NB, UK*
[2]*Department of Earth Sciences, University of Liverpool, Liverpool, L69 3BX, UK*

ABSTRACT: Backstripping is a technique employed to analyse the subsidence history of extensional basins, and involves the progressive removal of sediment loads, incorporating the isostatic and sediment decompaction responses to this unloading. The results of backstripping calculations using 1D models employing local (Airy) isostasy and 2D models employing 'flexural' isostasy are compared for three cross-sections of the North Sea rift basin. Backstripping is commonly used to estimate stretching factor (β) across extensional basins. At structural highs 1D Airy backstripping will overestimate β by comparison with predictions from 2D flexural backstripping, because Airy isostasy fails to acknowledge the effects of lateral differential loading. Predictions of β from 2D flexural backstripping are closer to those derived from forward modelling. 1D Airy backstripping also produces unrealistic internal deformation of individual fault-blocks and overestimates β when the pre-rift sequence is not fully decompacted.

The palaeobathymetric data required by 1D Airy backstripping are often inaccurate, which yields misleading results. 2D flexural backstripping has been formulated as reverse post-rift modelling, which is used to produce sequential (isostatically balanced) palinspastic post-rift cross-sections. These are calibrated using only high-quality palaeobathymetric data, allowing 2D flexural backstripping to be used to predict palaeobathymetry away from the calibration points.

KEYWORDS: *isostasy, flexure (geology), compaction (geology), subsidence, basin development*

INTRODUCTION

The aim of backstripping is to analyse the subsidence history of a basin by modelling a progressive reversal of the depositional process. While *sensu stricto* backstripping may be applied to any sedimentary basin (including platforms and foreland basins), it is most commonly applied to extensional basins, where it is used to determine the magnitude of lithosphere stretching from post-rift subsidence rate (Sclater & Christie 1980). In addition to constraining the magnitude of lithosphere stretching and resulting basement geotherm perturbations for hydrocarbon maturation modelling, backstripping may also be used to make predictions about geological features within a basin, such as palaeobathymetry and palaeotopography, (Roberts *et al.* 1993*b*, Kusznir *et al.* 1995, Nadin & Kusznir 1995, Roberts *et al.* 1997, Walker *et al.* 1997).

The backstripping procedure consists first of removing units of stratigraphy from the top downwards (hence backstripping). Corrections must also be made for sediment compaction in response to burial and for subsidence arising from the isostatic response to sediment loading. Palaeobathymetry estimates are needed in order to constrain or calibrate earlier stages of basin bathymetry. The isostatic response to loading is commonly calculated assuming Airy (1D) isostasy. The 'traditional' approach, by virtue that it was the first to be used (e.g. Steckler & Watts 1978), is to treat isostasy as a one-dimensional problem. 2D flexural backstripping was introduced by Watts *et al.* (1982). More recently, 3D flexural backstripping has been implemented (Watts & Torné 1992, Norris & Kusznir 1993). The fundamental difference between Airy isostasy, used in 1D modelling, and flexural isostasy, used in 2D or 3D modelling, is that in the 1D approach isostatic loads are compensated locally, i.e. immediately beneath the load, while with the flexural approach loads are distributed regionally. 3D backstripping should provide the most reliable results, however, its general applicability is hampered by the volume of detailed stratigraphic data (maps) needed. Lateral sampling at scales of 1 km or less can, however, readily be provided by 2D data (cross-sections) based on interpreted seismic lines.

In extensional basins subsidence histories produced by backstripping are usually interpreted in terms of the lithospheric-stretching model of McKenzie (1978), in which lithosphere stretching gives rise to crustal thinning and elevation of the geotherm. Typically the McKenzie lithosphere extension model assumes a rapid period of syn-rift extension, coincident with surface faulting, followed by a period of slower time-dependent post-rift subsidence, during which the thermal anomaly, associated with the elevated geotherm from rifting, cools in an exponential manner with a time constant of *c.* 65 Ma. This episode of post-rift thermal subsidence causes significant subsidence of the basin floor for 150–200 Ma after the rift event itself.

The aim of this paper is to review 1D Airy-isostatic and 2D flexural-isostatic backstripping techniques and to compare the

1354-0793/98/$10.00

results of backstripping three cross-sections from an extensional basin using both techniques. From this we aim to show how 2D backstripping using flexural isostasy produces more satisfactory geological predictions.

1D BACKSTRIPPING USING AIRY ISOSTASY

Airy (1D) backstripping uses 1D stratigraphic data obtained from a well or a point sample of a cross-section. When applied to the post-rift sequence of an extensional basin the Airy backstripping process consists of the following steps:

(1) A sediment-loaded basement subsidence curve is constructed from the initial stratigraphic data by removing each layer in the sequence in turn (Fig. 1a)
(2) The remaining underlying sediment units are then decompacted (Fig. 1b).
(3) As each layer is removed, the new sediment surface is set to a prescribed datum by assuming a depth of deposition for each stratigraphic interval, and, if desired, correcting sea-level for long-term eustatic changes (Fig. 1c).
(4) The sediment-loaded subsidence curve is corrected to an equivalent water-loaded subsidence curve (Fig. 1d). The loading correction from sediment to water is performed assuming 1D Airy (local) isostasy.

This procedure produces the history of water-loaded basement-driving subsidence. The water-loaded basement subsidence curve is usually compared with theoretical subsidence curves for specific values of β (stretching factor), produced by the instantaneous stretching model of McKenzie (1978). The best fit between the observationally-derived subsidence curve and a theoretical subsidence curve is used to estimate β at the point at which the subsidence analysis was performed. Corrections to the theoretical subsidence curve allowing for rifting of finite duration may be made (Jarvis & McKenzie 1980). Previous examples of 1D backstripping applied to the North Sea can be found in Sclater & Christie (1980), Barton & Wood (1984), Giltner (1987), White (1990) and White & Latin (1993).

LIMITATIONS OF 1D AIRY BACKSTRIPPING

Palaeobathymetry

The accuracy of any water-loaded, basement-driving-subsidence history derived from 1D Airy backstripping depends fundamentally on the quality and quantity of palaeobathymetry data available for stage 3 above in order to constrain water-depth estimates through time. While coals, carbonate reefs and erosion surfaces provide reliable estimates of palaeobathymetry, the use of fossil assemblages to estimate palaeo-water depths may carry very large errors, as in the case of the Cretaceous of the Northern North Sea (Bertram & Milton, 1989; Nadin & Kusznir, 1996). Basement subsidence history is usually estimated by fitting a curve through the basement subsidence determinations at each time point. The resulting basement subsidence history, shown schematically in Fig. 2a, is often complex. If errors in palaeo-water depth are underestimated, as is often the case, then the resulting basement subsidence curve is incorrect and misleading. It is important that only high quality palaeo-water depths with known errors (e.g. coals, reefs, erosion surfaces) are used to calibrate McKenzie post-rift thermal subsidence (Fig. 2b) and determine β stretching factors. This is particularly important when departures from McKenzie post-rift subsidence, such as

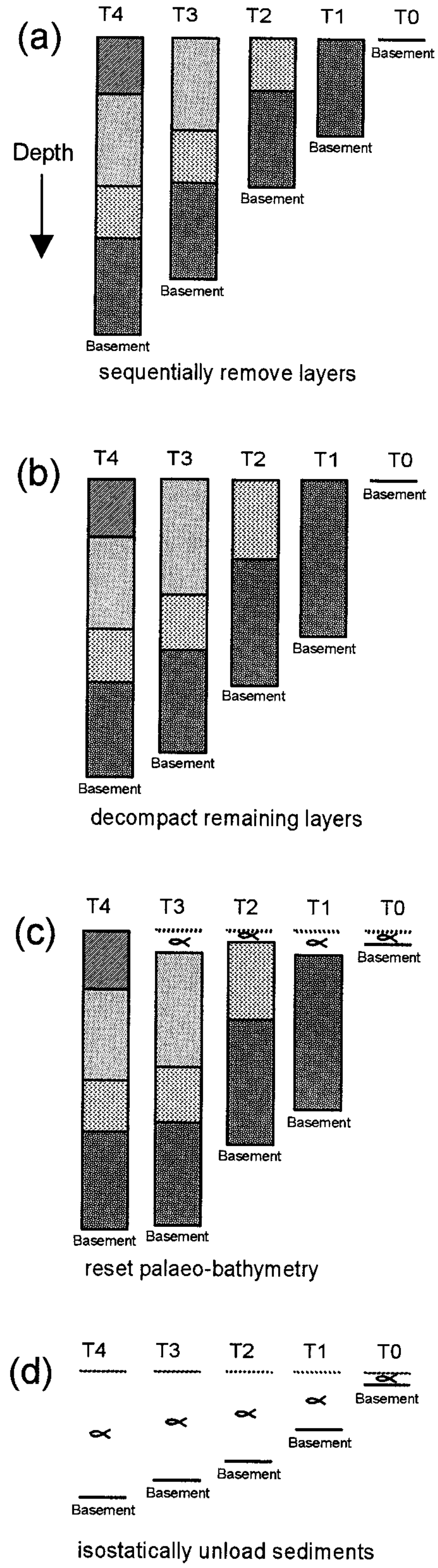

Fig. 1. Schematic illustration of the 1D Airy backstripping technique: (a) stratigraphic layers are progressively removed (top first); (b) remaining sedimentary layers are decompacted; (c) the top of the remaining decompacted section is reset to observed palaeobathymetry at each time stage; (d) the effects of sediment loading are removed using 1D local (Airy) isostasy in order to produce water-loaded basement-driving subsidence.

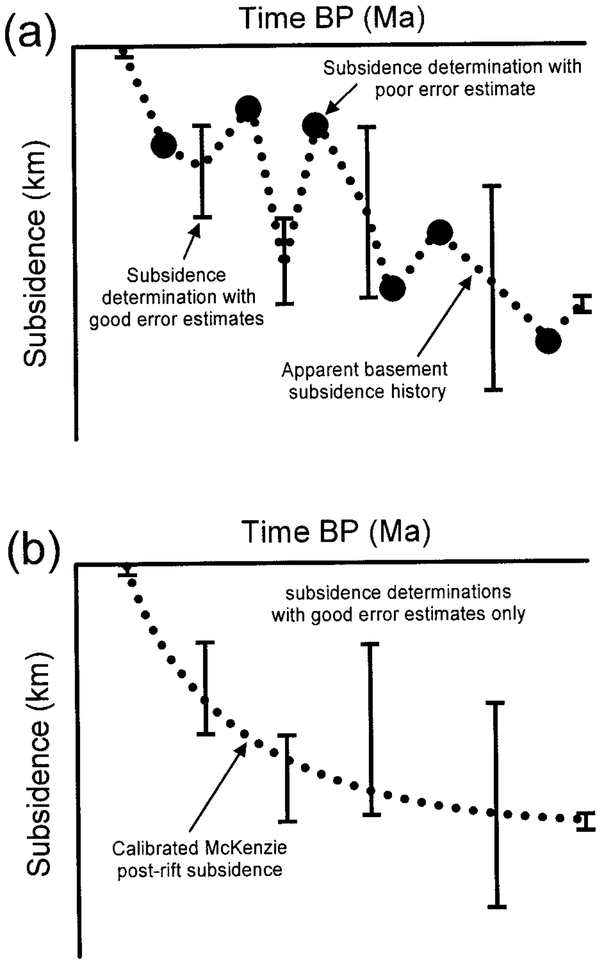

Fig. 2. The history of water-loaded basement-driving subsidence produced by 1D Airy backstripping is very dependent on the accuracy of observed palaeo-bathymetry at each time stage. (a) Inaccurate palaeobathymetry estimates give a complex but misleading subsidence history. (b) Only good quality palaeobathymetry estimates with quantified errors should be used to calibrate McKenzie post-rift subsidence and determine β.

occurred in the Northern North Sea during the Palaeocene (Bertram & Milton, 1989; Nadin & Kusznir 1995, 1996) are being identified and quantified.

Isostasy

Another critical assumption of 1D backstripping is that local (Airy) isostasy is a reliable approximation to the isostatic response of the lithosphere to loading. Local isostasy assumes that all loads are compensated by vertical movements beneath the load only, and that the magnitude of loads surrounding the sample point are irrelevant to its isostatic response. This is equivalent to assuming that the lithosphere has no elastic strength. In contrast, flexural isostasy assumes that any load on the lithosphere is also supported by flexural bending stresses within the immediate area surrounding the load. In geological terms, the finite flexural strength of the lithosphere means that any load, positive (i.e. deposition) or negative (i.e. erosion), has an effect on the subsidence/uplift history, not just vertically below the load, but also laterally around the load. For a given load the magnitude of vertical deflection under the load and its lateral wavelength are controlled by the flexural rigidity (D) of the lithosphere. As flexural rigidity is increased the width of the region experiencing a vertical deflection increases, while the amplitude of the deflection decreases. Analysis of the relationship between gravity and topography of young rifts (McKenzie & Fairhead 1997), gravity modelling of older extensional basins (Fowler & McKenzie 1989; Holliger & Klemperer 1990), and structural–stratigraphic forward modelling of the rifting process (Kusznir *et al.* 1991, 1995) demonstrate that rifted continental lithosphere possesses a finite long-term flexural strength.

Users of 1D Airy backstripping often acknowledge that the lithosphere has finite flexural strength but assume that a local (Airy) isostatic response can accurately approximate a flexural response with low effective elastic thickness (see next section for a formal description of this parameter). As we shall demonstrate in this paper, however, this assumption is invalid where the wavelengths of sediment loads are short, such as occurs for syn-rift or early post-rift sediment sequences deposited in half-grabens between rotated fault blocks. These fault blocks are typically 10–20 km wide and even for low values of effective elastic thickness (<3 km) we show that the subsidence on the fault block highs, where many wells are located, is influenced by sediment loading in the deeper intervening half-grabens.

The likely errors associated with the use of Airy isostasy for calculating the syn-rift and post-rift isostatic response to sediment loading have been examined and are outlined in the 'Discussion' section of this paper.

2D BACKSTRIPPING USING FLEXURAL ISOSTASY

The procedures used by 1D Airy backstripping, as described above, may be applied to a 2D cross section but with flexural rather than local isostasy being used to subtract sediment loading in order to determine basement-driving subsidence (Watts *et al.* 1982). While this overcomes the problems associated with the use of Airy isostasy in 1D backstripping, the problem of requiring good palaeobathymetry estimates remains; indeed the problem is compounded by now requiring profiles of palaeobathymetry at each time that basin-driving subsidence is to be determined. In order to overcome this problem Kusznir and co-workers (e.g. Roberts *et al.* 1993*b*; Hendrie *et al.* 1993; Kusznir *et al.* 1995; Nadin & Kusznir 1995, 1996) have advocated the use of a modified form of the flexural backstripping formulation, reverse post-rift thermal-subsidence modelling. This process produces a series of restored cross-sections whose validity can be tested or calibrated against observed palaeobathymetry.

The procedures involved in flexural reverse post-rift modelling a 2D cross-section are as follows (Fig. 3).

(1) The water layer at the top of the section is removed and the flexural isostatic response to this is computed.
(2) The uppermost stratigraphic unit of the section is then removed and the remaining sediment units are decompacted in response to this. Decompacted stratigraphic depths are referenced to the top of the basement.
(3) The flexural isostatic response to the removal of this sediment load from the section is calculated. Allowance is also made for the loading resulting from the increased porosity within the remaining stratigraphy.
(4) Thermal uplift (subsidence in reverse) is then added to the section from an estimate of β and rift age, using flexural isostasy and a 2D form of the McKenzie (1978) post-rift thermal subsidence model. In 1D modelling β is the principal derived variable, whereas in 2D modelling trial values of β are input to the calculations. In some circumstances constraints on the trial value(s) of β can be provided by forward modelling the syn-rift geometry of

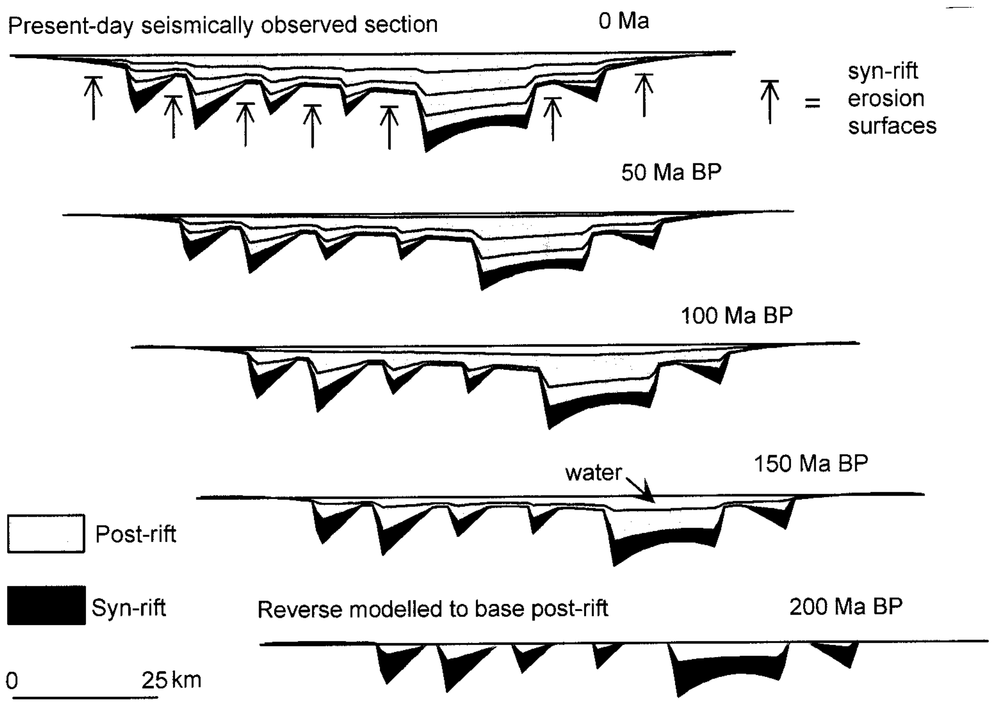

Fig. 3. Schematic illustration of 2D post-rift reverse modelling, consisting of flexural backstripping, decompaction and reverse thermal-subsidence modelling. Starting with a present-day depth section, sediment layers are successively removed to obtain a restoration at the base of the post-rift sequence. Sea-level markers, such as eroded fault-block crests, should be restored to sea-level.

the section (e.g. Roberts *et al.* 1993*b*; Kusznir *et al.* 1995; Nadin & Kusznir 1995), or by some other means of estimating tectonic extension from fault-block geometry.

(5) A correction is made, if required, for long-term eustatic variations in sea-level. The section is then water loaded once more, using flexural isostasy to compute the isostatic response.

(6) A palinspastically-restored (isostatically-balanced) cross-section is produced with the uppermost stratigraphic layer removed.

(7) The procedure in 1–6 is repeated for the remaining stratigraphic units, down to the base of the post-rift sequence (Fig. 3).

The above procedure provides a series of restored cross-sections which, in terms of their vertical elevation relative to sea-level, are dependent on the magnitude of β used in the reverse thermal subsidence calculations. An important test of the validity of 2D flexural backstripping is that stratigraphic surfaces once at sea-level should be restored to sea-level at the appropriate time in the model (Fig. 3). This is the geological control equivalent to the assumption of depositional water depth in 1D modelling. The best-fit restoration, constrained by palaeobathymetric data such as erosion surfaces, coals, sub-aerial lavas or limestone reefs, will be achieved using a particular value of β. In this way the flexural backstripping procedure may be used to determine a value for β.

Backstripping of cross-sections can be extended to embrace local (Airy) isostasy by setting flexural rigidity to zero ($T_e = 0$ km). In this instance a suite of restored sections is produced, but the isostatic calculations have operated only vertically, without consideration of laterally-adjacent loads (e.g. Roberts *et al.* 1993*b*, fig. 3e).

While the flexural strength of the lithosphere is strictly defined by its flexural rigidity (D), it is commonly expressed in terms of another variable, the effective elastic thickness (T_e), where

$$D = \frac{E T_e^3}{12(1-\nu^2)}$$

and E is Young's modulus and ν is Poisson's ratio. The effective elastic thickness is a notional parameter which describes the thickness of a perfectly-elastic layer with the same flexural strength as the lithosphere. Because the lithosphere is not perfectly elastic the depth to which bending stresses are carried within the lithosphere is much greater than the effective elastic thickness. T_e is, however, commonly used as a measure of lithospheric strength in preference to flexural rigidity because it has units of km, which are easier to visualize than the units of flexural rigidity, expressed in Nm. For example (using typical elastic parameters for granitic rocks) a flexural rigidity of *c.* 1.7×10^{20} Nm is equivalent to an effective elastic thickness of *c.* 3 km.

COMPARING THE RESULTS OF 1D AIRY AND 2D FLEXURAL BACKSTRIPPING

In two previous papers (Roberts *et al.* 1993*b*; Kusznir *et al.* 1995) brief comparisons were made of the results of 1D and 2D backstripping on the same section. It was claimed that 2D flexural isostasy yields the more realistic palinspastic restorations, and that the values of β predicted from flexural backstripping are closer to estimates of extension derived from other methods (e.g. forward modelling) than are estimates of β from Airy backstripping. In neither paper, however, was the sensitivity of the modelling the main topic discussed; rather the papers demonstrate the applicability of combined forward and reverse flexural modelling to geological examples. In this paper we explicitly investigate the sensitivity of backstripping geological cross-sections to changes both in flexural rigidity and values of β used for thermal modelling . This is done using three cross-sections which have previously been published and modelled: Viking Graben 1 – Roberts *et al.* (1993*b*, fig. 5);

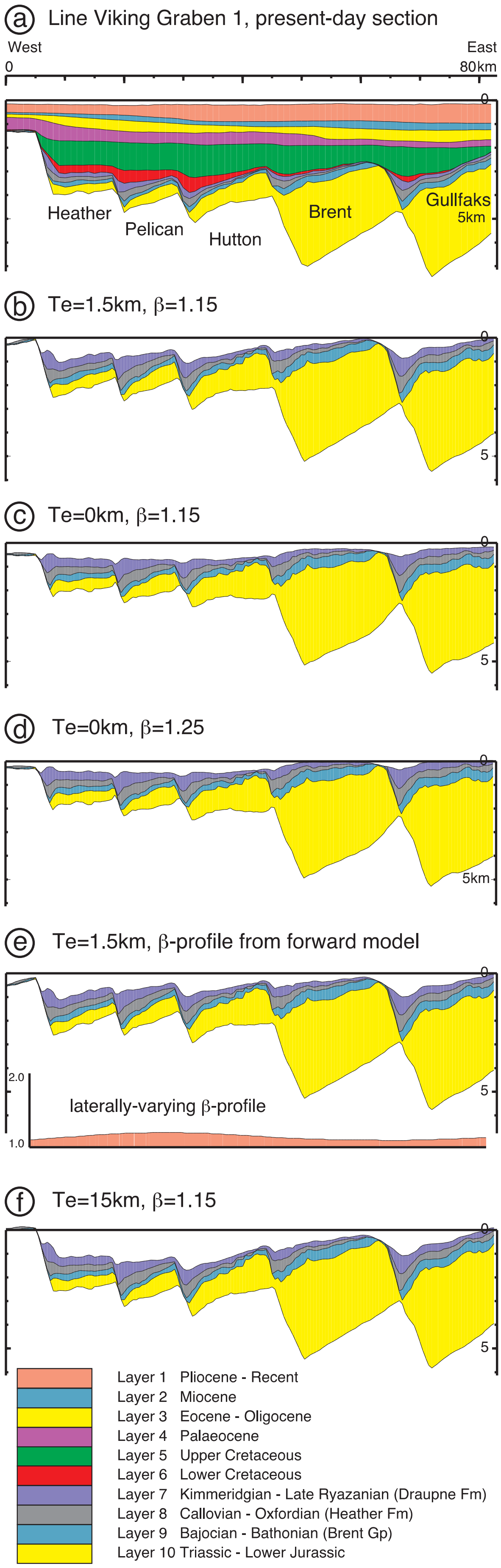

Fig. 4. Backstripped restorations of a profile crossing the East Shetland Basin in the Northern North Sea (line Viking Graben 1), vertically exaggerated for clarity. The names refer to major fault-blocks and do not indicate the precise location of hydrocarbon fields. (a) Present-day depth section. Upper six layers are Cretaceous–Quaternary post-rift, layers 7 & 8 are Upper Jurassic syn-rift, layers 9 & 10 are Jurassic and Triassic pre-rift. (b–f) Restorations to the base of the Cretaceous, derived using the combinations of β and T_e labelled on each plot.

Viking Graben 2 – White (1990, fig. 11.8); Central Graben – Roberts *et al.* (1993*b*, fig. 10). These lines can be geographically located in the earlier papers. For the purposes of this discussion their location is not of principal importance.

Viking Graben 1 (Fig. 4)

This line crosses the East Shetland Basin of the Northern Viking Graben in the North Sea (Roberts *et al.* 1993*b*, fig. 4). The line (Fig. 4a) crosses the basin margin in the west and five tilted fault-blocks of Late Jurassic age (Yielding *et al.* 1992; Roberts *et al.* 1993*a* & *b*). Note that thickness changes in the Triassic (at the base of the section) imply a Triassic rift history also (Roberts *et al.* 1995; Færseth 1996). Here, however, we are concerned with backstripping relative to the younger Late Jurassic event.

Figure 4a shows the present-day geometry of the cross-section; below this (Fig. 4b–f) are a series of restorations to the base of the Cretaceous (layers 1–6 removed), shortly after the cessation of extension in this area (Roberts *et al.* 1993*a*). In these restorations we test sensitivity to variations in effective elastic thickness (T_e), one of the principal parameters controlling the wavelength of the flexural–isostatic response. In all restorations decompaction follows the methodology of Sclater & Christie (1980), long-term eustasy follows the long-term curve of Haq *et al.* (1987), and we also incorporate the thermal effects of an earlier Triassic rift (250 Ma), magnitude $\beta = 1.2$ (see Giltner 1987; Roberts *et al.* 1995).

Figure 4b shows a base Cretaceous restoration of the line which has used a T_e of 1.5 km to control the flexural–isostatic response and a Late Jurassic (155 Ma) β of 1.15 to control the reverse thermal modelling. The choice of this low value for T_e stems from the work of Roberts *et al.* (1993*b*, 1995), whose sensitivity tests showed that a T_e of 1.5 km provides the best fit for combined forward and reverse modelling of fault-block erosion profiles in this area. In Fig. 4b the crest of the eroded basin margin has been returned to sea-level, as has the crest of the Brent fault-block and the illustrated part of the Gullfaks block. The critical bathymetric control point is the crest of the Brent block, which stratigraphic data show should be at, or just below, wave-base at this time (Livera & Gdula 1990; Roberts *et al.* 1993*a*). The illustrated restoration of Brent is thus geologically satisfactory. The crest of the Gullfaks block should probably be emergent at this time (Spencer & Larsen 1990). Our restoration restores the down-dip flank to sea-level and is thus geologically satisfactory. (Other unpublished restorations show the crest of Gullfaks emergent throughout the Early Cretaceous.) Returning the eroded basin margin (west) close to sea-level is also taken to be acceptable, although no precise stratigraphic data are available here. There is no record of significant erosion on the smaller Heather, Pelican and Hutton fault-blocks and thus their restoration below sea-level is in accordance with geological data.

Figure 4b can tell us a number of things. First, from the perspective of basin modelling, the geological acceptability of the restoration means that the choice of T_e may be reasonable.

An estimate of Late Jurassic β of 1.15 may also be acceptable. Second, from the geological perspective, the restoration allows us to make predictions about palaeobathymetry and potential depocentres, together with an assessment of which structures may, through emergence, have acted as a source for syn-rift/early post-rift reservoir. This would not be possible from 1D backstripping of well data.

Figure 4c shows a second base Cretaceous restoration. The only difference between the model used here and that of Fig. 4b, is that T_e (and thus flexural rigidity) has been set to zero (i.e. Airy isostasy). There are some clear differences between Figs 4b & c. In Fig. 4c no part of the section is returned to sea-level and the internal geometry of the fault-blocks has changed, with much of the differential sea-floor bathymetry present in Fig. 4b having been removed.

The internal change of fault-block shape is not thought to model a real geological process. It is considered an artefact of Airy isostasy. Airy isostasy does not acknowledge lateral differential loading and as a consequence results in restorations of structural highs (e.g. fault-block crests) which are too deep and restorations of structural lows which are too shallow, thus removing much of the internal topography of the fault-blocks. This arises because when finite flexural rigidity is acknowledged (e.g. Fig. 4b) the subsidence history of a given structural high is controlled not just by loading from above, it is amplified by loading from the adjacent hanging wall and dip-slope depocentres. Conversely, the subsidence history of a given structural low is controlled both by vertical loading from above and the reduced loading on the adjacent structural high and dip-slope. When this lateral loading effect (the 'sideways glance' of the title of this article) is not acknowledged (Airy isostasy) the fault-blocks deform internally (by vertical simple shear) during restoration, demonstrating that Airy isostasy is not a realistic model of lithosphere loading during post-rift subsidence.

Using 1D sample data (e.g. well data) internal fault-block deformation cannot be seen. It is primarily for this reason that this shortcoming of 1D backstripping has not previously been highlighted.

Figure 4d shows a similar restoration to Fig. 4c, but the magnitude of the Late Jurassic β-factor has been increased to 1.25 (i.e. an increase in extension of 66%). In this restoration the crest of Brent is just below sea-level and the flank of Gullfaks is very slightly emergent. The restoration, however, still suffers from internal deformation of the fault-blocks, and there is now the question of whether $\beta = 1.25$ is realistic for the fault geometries on this line.

This question can be answered by forward modelling. Roberts *et al.* (1993*b*, fig. 5) illustrated a flexural-cantilever forward model (Kusznir *et al.* 1991) of this line, matching the model to a backstripped template. The β-profile produced by the forward model is shown in Fig. 4e, together with a base Cretaceous restoration which used the β-profile to constrain reverse thermal modelling. T_e for this model was 1.5 km. Comparison of Figs 4b & 4e shows them to be similar. This is because the β-profile from the forward model encompasses the range 1.1–1.2, the mean value being about 1.15, the constant value used to restore Fig. 2b. Most importantly, the forward-modelled β-profile nowhere reaches a value of 1.25, yet this is the value of β required to restore the crest of Brent, the flank of Gullfaks and the platform margin close to sea-level if Airy isostasy is assumed (Fig. 4d). This suggests that not only is an Airy restoration geometrically inferior to a flexural restoration with a small-but-finite T_e (1.5 km) but that a satisfactory palaeobathymetric fit is only achieved by using a value of β which is not compatible with the fault geometry on the same line.

Figure 4f is the final base Cretaceous restoration of line Viking Graben 1. As in 4b and 4c a constant β of 1.15 has been used, but in 4f a large T_e of 15 km has constrained flexural isostasy. This value of T_e would correspond to perfect elasticity for the thickness of the entire upper crustal seismogenic layer in normal continental lithosphere (e.g. Jackson 1987). Comparing Fig. 4f with 4b and 4c, it is clear that the geometry of 4f is more similar to 4b, the main difference being an increased bathymetry over the central part of the section. We believe the geometry of Fig. 4f to be more acceptable than the Airy restoration in Fig. 4c and suggest that while the restoration of this line is sensitive to the value of T_e, the critical issue is not the exact value but whether T_e is 0 km or is finite. Iterative modelling has led us to conclude that a T_e of 1.5–3 km provides the best results in this area. We suggest that a T_e of 0 km is unacceptable.

Viking Graben 2 (Fig. 5)

This line also runs *c.* W–E across the East Shetland Basin, slightly oblique to line Viking Graben 1, intersecting it on the Brent fault-block. This line has previously been used for Airy backstripping by White (1990, see his fig. 2 for location and fig. 8 for illustration). Our redisplay of this line (Fig. 5a) is slightly different from White's original interpretation in that, using the seismic and well data from the area, we have interpreted the likely top of crystalline basement (base Triassic) (see also Roberts *et al.* 1995; Færseth 1996). White stopped his interpretation at the base of the Jurassic. This line is sufficiently close to Viking Graben 1 (Fig. 4) that we should expect the results from analysis of Viking Graben 1 to be broadly reproducible on this second line.

Figure 5b shows Viking Graben 2 backstripped to the base of the Cretaceous using a T_e of 1.5 km and a Late Jurassic (155 Ma) β of 1.15. In this model, and all others of this line, a Triassic (250 Ma) β of 1.2 is assumed. The controlling parameters on Fig. 5b are thus identical to those of Fig. 4b. The restoration of the two sections is also similar. In both cases the basin margin (west) is restored to sea-level, as is the crest of the Brent fault-block. The intervening fault-blocks (Cormorant & Hutton in Fig. 5b) are fully submarine in both models. East of Brent the crests of the Rimfaks & Gullfaks Sør fault-blocks are restored to sea-level in Fig. 5b. All of the structures at sea-level in Fig. 5b have eroded crests and their restoration to sea-level is therefore consistent with palaeobathymetric information. There is thus also consistency between two comparable flexural models of lines Viking Graben 1 and 2.

Figure 5c shows Viking Graben 2 backstripped to the base Cretaceous using a T_e of 0 km and a constant Late Jurassic of 1.25. The controlling parameters are thus the same as for Fig. 4d. The crests of the Brent and Rimfaks fault-blocks are restored to sea-level but, as with the Airy models of Viking Graben 1, significant internal deformation of all the fault-blocks has occurred during the reverse modelling. The restoration in Fig. 5c is less satisfactory than that in Fig. 5b. Flexural isostasy, even with a T_e as low as 1.5 km, is required to maintain the relief between structural highs and lows during backstripping.

Figure 4e showed that a β-profile produced by forward modelling line Viking Graben 1 is compatible with flexural backstripping of the same line, but is incompatible with the Airy backstripped model, the latter requiring higher β values. We have constructed many forward models across the East Shetland Basin. None have produced estimates of Jurassic β exceeding 1.2 and in general β does not exceed 1.15. There is thus no independent justification for the β of 1.25 required to restore the fault-block crests in Fig. 5c.

White (1990) performed 1D backstripping on six sample points from line Viking Graben 2, one from each fault-block. While we estimate a constant β for the profile to be *c.* 1.15 (Fig. 5b), White estimated the range in Jurassic β to be 1.19–1.31, with a mean value of 1.25. This result appears consistent with our own Airy backstripping of the line (Fig. 5c). White, however, realized that 1D backstripping yields over-estimates of β when performed on samples from structural highs. He therefore sensibly sampled the mid-points of the fault-blocks in an attempt to avoid a structural sampling bias. All other assumptions being the same, Airy backstripping of fault-block mid-points should yield similar estimates of β to flexural backstripping, the loading effects of the adjacent highs and lows tending to cancel out. Why then did White obtain an estimate of Jurassic extension *c.* 66% greater than our own? The reason lies in the decompaction assumptions. White did not extend his seismic interpretation significantly into the pre-rift, stopping at the top Triassic. He therefore assumed that all pre-Late Jurassic sediments were fully compacted (i.e. had zero porosity) prior to Late Jurassic extension. This is not a viable assumption in the Northern Viking Graben, because oil is produced from primary porosity in Triassic sandstone reservoirs (e.g. Snorre field, Hollander 1987; Dahl & Solli 1993).

Figure 5d shows the effect on backstripping line Viking Graben 2 ($T_e = 1.5$ km) when the Triassic is assumed to have no porosity at the beginning of the Cretaceous. In order to restore the crests of the Brent and Rimfaks fault-blocks to sea-level a Late Jurassic β of 1.3 is required, i.e. the predicted extension is twice that of the flexural model in which the Triassic was decompacted (Fig. 5b). We believe this prediction of β to be unsustainable by forward modelling and suggest that the assumptions in the decompaction scheme must be wrong. We prefer to involve the full sediment column in decompaction, rather than stop decompacting within the pre-rift stratigraphy. This explains why White's estimates of Jurassic β for this line were larger than our own.

Figure 5e shows the final restoration of Viking Graben 2. Airy isostasy has been assumed and the Triassic has not been decompacted. The geometry of the section is highly distorted and in order to restore the crest of the Brent block to sea-level a β of 1.45 is required, an extension estimate (45%) three times that of Fig. 5b. This is an unacceptable amount of Jurassic extension for this area and serves to highlight the dangers of inaccurate geological input during backstripping.

Central Graben (Fig. 6)

This section crosses the Central Graben of the North Sea, *c.* 400 km south of the previous lines. It was interpreted and forward modelled by Price *et al.* (1993, fig. 3, located on their fig. 1) and backstripped by Roberts *et al.* (1993*b*, fig. 10). The sensitivity of this line to assumptions in backstripping has not previously been investigated. The line provides a number of features to observe during backstripping (Fig. 6a). In the western footwall of the Graben is the Forth Approaches Platform (Platform on Fig. 6a) and in the eastern footwall is the Jæren High; both are thought to be eroded at the base of the Cretaceous following footwall uplift on the graben boundary faults (Roberts *et al.* 1990; Price *et al.* 1993). The Central Graben itself comprises two Late Jurassic basins, the symmetric West Forties Basin and the asymmetric East Forties Basin, separated by the eroded Forties–Montrose High. This high is also an uplifted and eroded Late Jurassic footwall (Price *et al.* 1993, fig. 4). The aim of backstripping this line is to restore the eroded basin margins and the Forties–Montrose High to sea-level at the time of Late Jurassic extension (*c.* 155 Ma). The Triassic locally overlies mobile Zechstein salt which adds structural complexity to this section not seen in the Viking Graben.

Triassic extension has not been explicitly quantified in this area, but the presence of a regionally-thick Triassic sequence in the Central Graben (e.g. Sørensen 1986; Lervik *et al.* 1989) suggests that Triassic extension was not negligible. We have assumed a Triassic β of 1.2, as in our Viking Graben models (see also Roberts *et al.* 1995). All models incorporate long-term eustasy (after Haq *et al.* 1987).

The end syn-rift restoration of this line shown in Fig. 6b is a flexural model. It has been backstripped to the base of layer 4 (155 Ma) using a T_e of 1.5 km and a constant Late Jurassic β of 1.2. The eroded platforms flanking the graben are restored to sea-level, but the eroded Forties–Montrose High is left with a bathymetry of a few hundred metres. This is rectified in Fig. 6c, which uses a laterally-varying β-profile (1.2 at the margins, 1.3 in the centre) to constrain reverse thermal modelling. This β-profile is not constrained by forward modelling, it is simply a best-fit profile for restoring the eroded structures to sea-level. Figure 6c is geologically acceptable.

Although parts of the section are restored to sea-level in Fig. 6c, other areas show appreciable bathymetry (>1 km in the East and West Forties Basins), in which it should have been possible to deposit syn-rift reservoir sandstones (Roberts *et al.* 1990; Price *et al.* 1993). The salt-cored anticlines of the West Forties Basin are also very prominent. These salt structures grew during the Late Jurassic, perhaps triggered by extension in the basement (Roberts *et al.* 1990) and their relief is probably exaggerated at the time of the restoration. Nevertheless monitoring the way in which these short-wavelength/high-amplitude structures respond to different backstripping assumptions is informative.

Figure 6d shows a restoration produced using Airy isostasy, with other assumptions the same as Fig. 6c. Nowhere on this section has been returned to sea-level, indicating that Airy backstripping of the structural highs will require a higher β than the comparable flexural model for satisfactory restoration. There are, however, more fundamental differences between Figs 6c & 6d, notably the overall geometry of the sections. Airy backstripping has imposed substantial internal deformation of the fault-blocks and basins during restoration. The results of this are that the East Forties Basin (hanging wall of the Jæren High) has disappeared, the sea-floor topography in the West Forties Basin has been reduced and the central Forties–Montrose High now lies below the adjacent basinal areas. The distortion of the salt-induced topography in the West Forties Basin has also resulted in deformation of the base-salt/top-basement interface. None of this distortion of internal structure is likely to reflect real geological deformation during post-rift burial, rather it is an artefact of backstripping with Airy isostasy. This would not be apparent if 1D sample data had been used.

Figure 6e shows a second Airy restoration of the Central Graben line, produced using a constant Jurassic β of 1.4. This restoration still shows internal deformation imposed during backstripping, but it does restore the eroded basin margins to sea-level. The 'penalty' for this is the much higher value of β that has been used by comparison with flexural restoration of the basin margins. The forward modelling of extension in the Central Graben is more difficult than in the Viking Graben, because the Permian salt acts to decouple much of the deformation in the basin fill from true crustal extension in the sub-salt basement. Nevertheless two simple forward models of

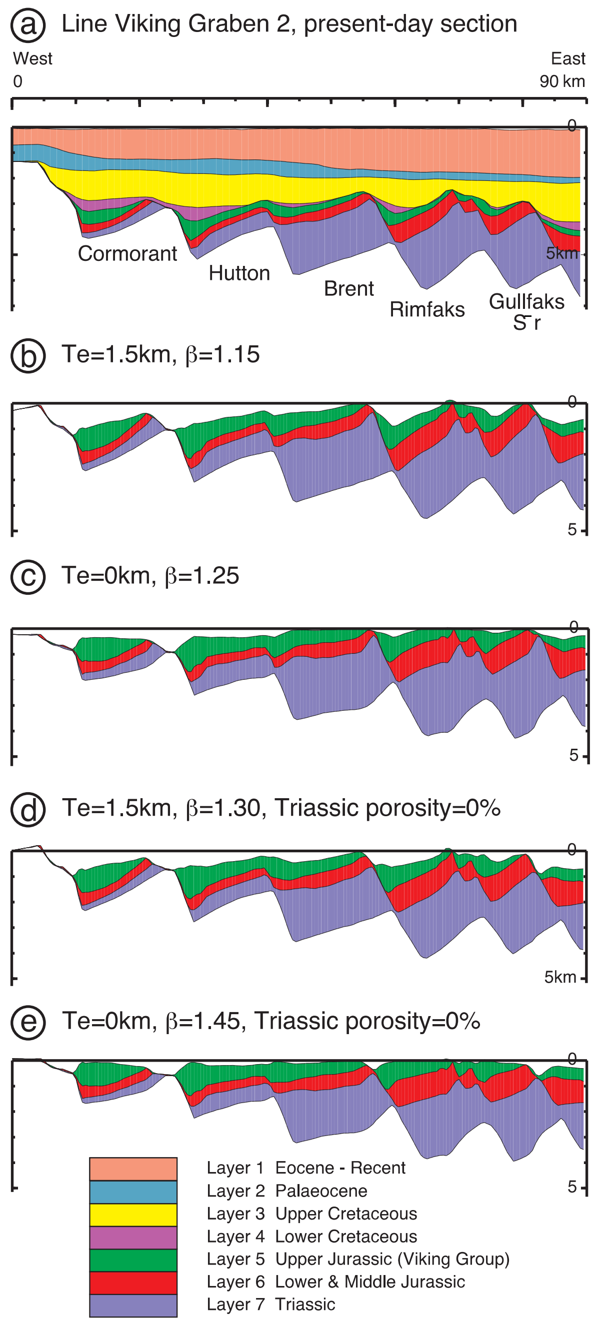

Fig. 5. Backstripped restorations of a profile crossing the East Shetland Basin in the Northern North Sea (line Viking Graben 2), vertically exaggerated for clarity. The names refer to major fault-blocks and do not indicate the precise location of hydrocarbon fields. (a) Present-day depth section. Upper four layers are Cretaceous–Quaternary post-rift, layer 5 is Upper Jurassic syn-rift, layers 6 & 7 are Jurassic and Triassic pre-rift. (b–e) Restorations to the base of the Cretaceous, derived using the combinations of β, T_e and porosity labelled on each plot.

this line have previously been published (Price *et al.* 1993 (model by AMR); Hendrie *et al.* 1993). The Jurassic β-profiles from these models have maximum values of 1.15 and 1.23, respectively. These may be underestimates of the true maximum Jurassic β in this area, because of the problem of seismic imaging below the salt. They are not, however, likely to be underestimates by a factor of *c.* 2, which is what the restoration in Fig. 6e implies. The β required by Airy backstripping of the

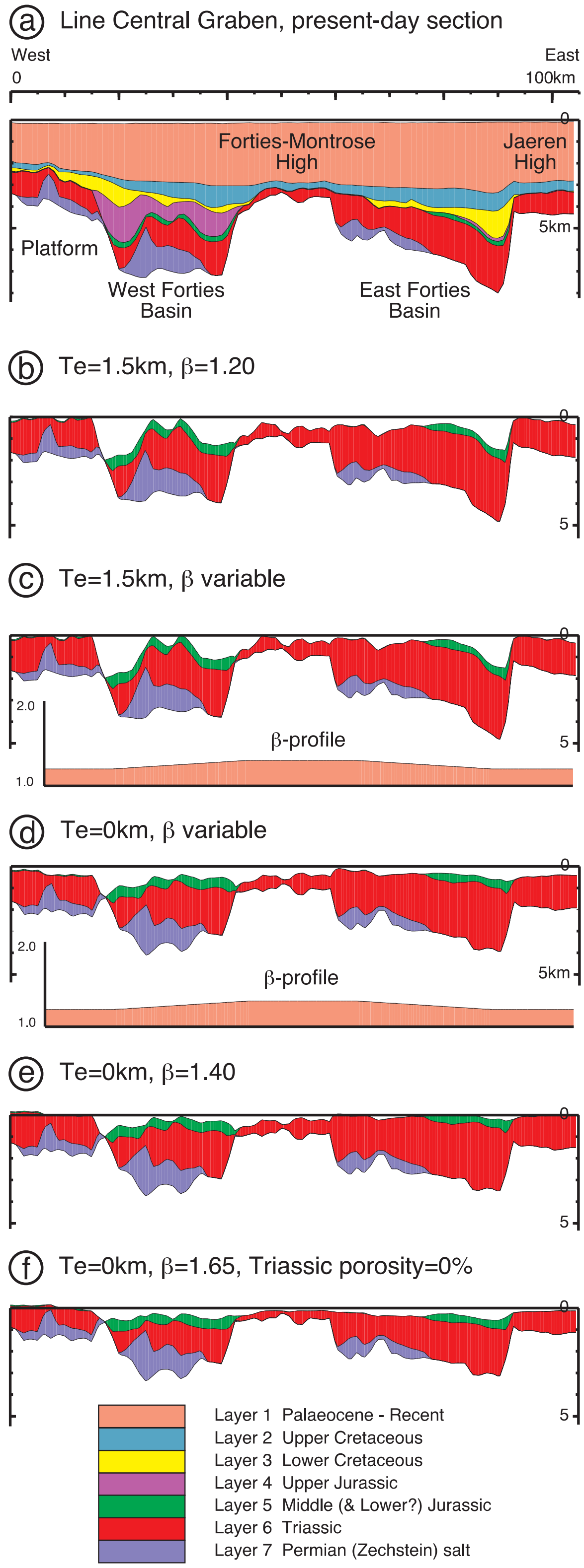

Fig. 6. Backstripped restorations of a profile crossing the Central Graben (Central North Sea), vertically exaggerated for clarity. (a) Present-day depth section. Upper three layers are Cretaceous–Quaternary post-rift, layer 4 is Upper Jurassic syn-rift, layers 5 & 6 are Jurassic and Triassic pre-rift, layer 7 is mobile Permian salt. (b–f) Restorations to the Late Jurassic (155 Ma, syn-rift), derived using the combinations of β, T_e and porosity labelled on each plot.

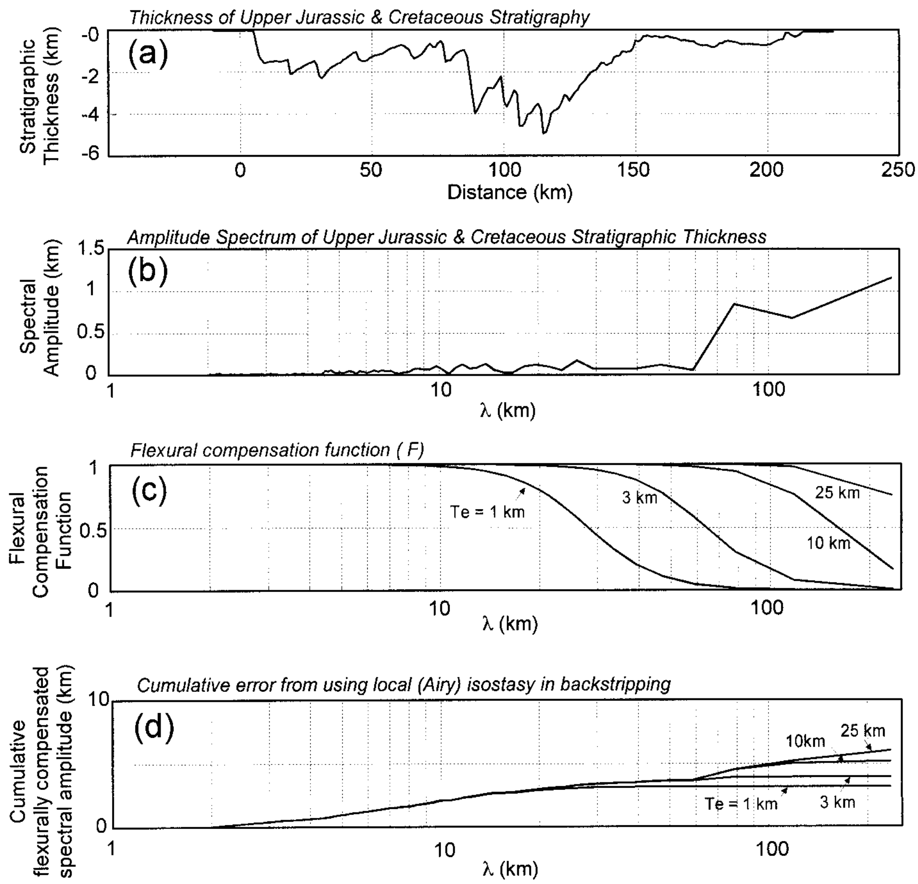

Fig. 7. Analysis of the spectral content of syn-rift and early post-rift sediment loading and its flexural isostatic response. (a) Thickness profile of Upper Jurassic (syn-rift) and Cretaceous (early post-rift) across the North Viking Graben. (b) Amplitude spectrum of Upper Jurassic–Cretaceous thickness as a function of wavelength. (c) Flexural compensation function, *F*, (also called complementary isostatic compensation function, see text) as a function of wavelength for $T_e = 1$, 3, 10 and 25 km. (d) Cumulative summation of harmonic amplitudes for the product of the amplitude spectrum of Upper Jurassic and Cretaceous thickness and the complimentary isostatic compensation function, *F*, as a function of wavelength. This product and its cumulative summation show the significant errors arising from the use of local (Airy) isostasy to determine the isostatic response to sediment loading. Flexural isostasy should be used instead.

structural highs on this line is thus too high to be consistent with the observed fault-block geometries.

The final restoration of the Central Graben profile (Fig. 6f) is similar in its construction to the final restoration of line Viking Graben 2 (Fig. 5e). It has been derived using Airy isostasy and without decompacting the Triassic. (The salt is not decompacted in any restoration). A constant Jurassic β of 1.65 has been used. The Forth Approaches Platform is restored to sea-level, the Forties–Montrose and Jæren Highs are just below sea-level. There has once more been considerable internal deformation imposed during the backstripping. The additional penalty of the restoration is the unacceptably high β that has been used in order to honour sea-level markers on the structural highs. At the rift flanks the β of 1.65 implies a required extension more than three times greater than that implied by our preferred flexural model ($\beta = 1.2$, Fig. 6b & c).

In view of the discussion above, the assumptions used for backstripping to Fig. 6f might seem unacceptably simple. The combined assumptions of Airy isostasy and non-compacting pre-rift are, however, often made in 1D backstripping studies. Figure 6a lies within the bounds of a regional 1D backstripping study in the Central North Sea (White & Latin 1993). The White & Latin study, which used a large number of exploration wells, adopted the assumptions of Airy isostasy and non-compacting pre-rift (Triassic). While the sample of wells in the study was selected in order to attempt to avoid a structural sampling bias, this is unlikely to have been achieved as exploration companies have not drilled structural lows in this area. The well-derived 1D data used for this study were therefore unavoidably biased towards structural highs, some of which are salt cored. In their study of sensitivities White & Latin (fig. 2) demonstrated that ignoring decompaction of the Triassic in this area can lead to an overestimation of Jurassic extension by as much as 66–100%, much as we have shown. In the remainder of their analyses, however, no decompaction of the Triassic was performed and yet they argued that their estimates of Jurassic β were likely minima once all variables were considered.

In the Central Graben, White & Latin estimated Jurassic β in the graben axis to be in the range 1.5–1.75 (their fig. 9). This range brackets our own estimate of $\beta = 1.65$, derived from the same assumptions (Fig. 6f). We believe this to be an overestimate of Jurassic β.

DISCUSSION

In this paper we have compared and contrasted the results of 1D Airy and 2D flexural backstripping, as applied to three cross-sections from the North Sea. We believe that 2D flexural backstripping gives more reliable predictions than the corresponding 1D Airy backstripping technique. The reasons for this are apparent from a spectral analysis of syn-rift and early post-rift loads across a full transect of the northern Viking Graben.

Lateral variations in the present-day thickness of the syn-rift (Upper Jurassic) and early post-rift (Cretaceous, Upper & Lower) stratigraphic units across a profile from the northern Viking Graben are shown in Fig. 7a (see Nadin & Kusznir 1995, fig. 11 for original profile). The saw-tooth thickness variations, with wavelengths 10–20 km, reflect the control by extensional faulting and rotated fault block geometry on both Late Jurassic and Early Cretaceous deposition. The total width of the rift system is of the order of 200 km. Basin fill generates an isostatic response by sediment loading; the sediment load due to stratigraphy of Late Jurassic and Cretaceous age is proportional to the thickness shown in Fig. 7a.

An amplitude spectrum of these thickness variations is shown in Fig. 7b, in which spectral amplitude is plotted against wavelength, λ. The largest amplitude values occur for $\lambda \sim 100$ km and are associated with the main rift basin feature. The smaller amplitude components with $\lambda \sim 5$–30 km are associated with the rotated fault-blocks. The amplitude spectrum shown in Fig. 7b is proportional to the amplitude spectrum of the sediment load due to Upper Jurassic and Cretaceous stratigraphy. While the relationship between thickness and load is not linear because of compaction, compaction effects do not significantly change the shape of the spectrum shown in Fig. 7b. For simplicity the effects of compaction have been omitted in this analysis.

The isostatic compensation function, *C*, describes the ratio of the vertical isostatic deflection of a lithosphere plate, with combined flexural strength and isostatic restoring force, to that of a purely local (Airy) isostatic model for a periodic load of wavelength, λ, acting on the surface of the lithosphere (Turcotte & Schubert 1982). *C* is given by

$$C=\{(\rho_m-\rho_i)g\}/\{(\rho_m-\rho_i)g+Dk^4)\}$$

where *D* is the flexural strength of the lithosphere, *k* is wavenumber ($k=2\pi/\lambda$), ρ_m is mantle density, ρ_i is surface infill density (water or sediment) and *g* is gravitational acceleration. The fraction of the periodic load that is regionally supported by flexural isostasy may be defined by a complementary isostatic compensation function, *F*, given by:

$$F=1-C$$

$$=1-\{(\rho_m-\rho_i)g\}/\{(\rho_m-\rho_i)g+Dk^4)\}$$

The complementary isostatic compensation function, *F*, is shown in Fig. 7c (labelled flexural compensation function) as a function of λ for a range of lithosphere flexural rigidities corresponding to values of effective elastic thickness, $T_e=1$, 3, 10 and 25 km . Values of Young's modulus $E=10^{11}$ N m^{-2}, Poisson's ratio $=0.25$, $\rho_m=3300$ kg m^{-3} and $\rho_i=1000$ kg m^{-3} (water infill) have been used. For $T_e=3$ km and greater, loads of $\lambda<60$ km are more than 50% compensated by flexural isostasy, i.e. they are less than 50% compensated by local (Airy) isostasy. Spectral amplitudes at these wavelengths of <60 km are predominantly associated with the fault-controlled saw-tooth thickness variations of the Upper Jurassic and Lower Cretaceous. Even for a T_e as low as 1 km, 50% of load is flexurally compensated for $\lambda=30$ km. For $T_e>10$ km most of the load of Jurassic–Cretaceous thickness variation is compensated flexurally for the whole of the basin. The use of a larger infill density (ρ_i) than for water (e.g. sediment density) has the effect of increasing *F*.

Amplitude spectra, as shown in Fig. 7b, under-emphasize the contribution of low wavelength components to total thickness and load. Significant contributions to total thickness (and load) arise from the large number of short wavelength harmonics. The cumulative summation of harmonic amplitudes, for the product of the thickness amplitude spectrum of the Jurassic–Cretaceous sediment thickness and the complimentary isostatic compensation function *F*, is shown in Fig. 7d. This product describes the error, as a function of λ, which would be generated if local (Airy) isostasy were used to predict the isostatic response to sediment loading rather than flexural isostasy. Its cumulative summation allows the important contributions of the large number of short wavelengths harmonics to be accounted for. Cumulative error is shown for $T_e=1$ km, 3, 10 and 25 km used to define lithosphere strength. Errors increase as the actual flexural strength of the lithosphere increases and are most severe for the curve for $T_e=25$ km when most of the basin is flexurally compensated (see Fig. 7c). The curve for $T_e=1$ km shows, however, that significant errors still arise from the use of local (Airy) isostasy even for low T_e values, especially for small wavelengths (i.e. for $\lambda<20$ km when $T_e=1$ km).

Estimates of T_e for rifted lithosphere while small are finite. Forward structural and stratigraphic modelling gives values in the range $T_e=1.5$–5 km (Roberts *et al.* 1993*b*; Magnavita *et al.* 1994; Kusznir *et al.* 1995). Admittance and coherence studies of the relationship between gravity and topography predict values in the range $T_e=2$–10 km (Hayward & Ebinger 1996; McKenzie & Fairhead 1997). Backstripping sediment loading, as in the case of the Northern North Sea Basin profiles described in this paper, is therefore invalid using Airy isostasy ($T_e=0$ km). Flexural isostasy should be used instead.

There are, however, some circumstances in which the results of 1D backstripping will approach those of the comparable 2D flexural technique. If the loads in a basin have a long wavelength (e.g. $\lambda>100$ km for $T_e=3$ km), then the effects of lateral differential loading will be minimal and the difference between 1D and 2D models of such loads will also be small. In a rift basin the syn-rift and early post-rift basin floor will typically be influenced by short-wavelength fault-block topography. At this time the effects of differential lateral loading will be at a maximum and the need to use a flexural model for backstripping will be greatest. As the rift-induced topography is filled then the lateral variation in loading will become more subdued and the results of 1D and 2D isostatic modelling will begin to converge. It is for this reason that some who have used an Airy model for backstripping the younger part of a post-rift sequence (e.g. Barton & Wood 1984), claim there to be little difference in the predictions of Airy and flexural backstripping when T_e is low. To yield the most reliable results, backstripping must, however, proceed using flexural isostasy through the full post-rift sequence.

In addition we have also reviewed the limitations placed on 1D Airy backstripping by the requirement of accurate palaeobathymetry at all times. The incorporation of flexural backstripping into a reverse post-rift modelling scheme which produces a series of restored cross-sections allows for a more efficient use of palaeobathymetric data; palaeobathymetry estimates at different times and locations on a 2D section may be used. Restored cross-sections produced using reverse post-rift modelling may only be calibrated using accurate palaeobathymetric estimates, such as coals, carbonate reefs and erosion surfaces.

CONCLUSIONS

(1) When backstripping structural highs, 1D Airy backstripping will yield higher estimates of β than 2D flexural backstripping. This is because Airy isostasy cannot acknowledge the effects of laterally-varying loads, in particular the loading of depocentres adjacent to structural highs. Estimates of extension using 1D Airy backstripping may be twice as much as from 2D flexural backstripping. There are clear implications for thermal modelling in the discrepancy of such results, particularly so given that most well data from rift basins are collected from structurally high locations.

(2) The predictions of β derived from flexurally-backstripped models are more in accordance with predictions of β from

forward modelling than are the predictions of 1D Airy backstripped models.

(3) 1D backstripping can only analyse 1D data, such as wells or vertical stratigraphic samples. 2D backstripping can be used to analyse geological cross-sections.

(4) 1D backstripping yields modelled subsidence curves as its primary output. 2D backstripping can also be used to produce subsidence curves, but its primary output of a sequence of palinspastically-restored cross-sections, predicting bathymetry and emergence through the post-rift history of a basin, provides more information on the basin evolution than do the simple subsidence curves.

(5) 2D flexural backstripping may be formulated as a reverse post-rift modelling process which produces a series of isostatically-balanced, restored cross-sections. These restored cross-sections are calibrated using only high quality palaeobathymetric estimates, thus providing more accurate estimates of β stretching factors.

(6) 1D Airy backstripping, when applied as a series of 1D samples across a cross-section, produces unrealistic distortion of internal fault-block geometries, that would not be recognized when isolated samples are analysed. Flexural backstripping maintains the internal geometry of fault-blocks.

(7) When incomplete decompaction of the pre-rift stratigraphy is performed then this too leads to overestimation of β, with extension estimates from incomplete decompaction being up to twice as large as estimates from a fully decompacted stratigraphic sequence.

(8) If 1-D Airy backstripping is combined with incomplete decompaction of the pre-rift, then extension estimates may be three times larger than those derived from a fully decompacted flexural model.

(9) Even if T_e is low (e.g. the 1.5 km used here) 2D flexural backstripping should always be superior in its predictions to Airy backstripping, because a 2D, rather than 1D, treatment of a 3D problem is being applied. The use of a flexural model is most critical when short-wavelength topography or short-wavelength loads are analysed. Flexural and Airy models start to converge when more regionally distributed loads are considered.

(10) The accuracy of the results of 1D Airy backstripping are very dependent on the quality of palaeobathymetric estimates required by the Airy backstripping process. As a consequence the predictions of Airy backstripping are often complex and may produce misleading estimates of β stretching factor.

We thank Kai Sørensen for his review and Tony Spencer for his editorial assistance. The corresponding author is Alan Roberts (email: alan@badleys.co.uk).

REFERENCES

BARTON, P. & WOOD, R. 1984. Tectonic evolution of the North Sea basin: crustal stretching and subsidence. *Geophysical Journal of the Royal Astronomical Society*, 79, 987–1022.

BERTRAM, G. T. & MILTON, N. J. 1989. Reconstructing basin evolution from sedimentary thickness; the importance of palaeobathymetric control, with reference to the North Sea. *Basin Research*, 1, 247–257.

DAHL, N. & SOLLI, T. 1993. The structural evolution of the Snorre Field and surrounding areas. *In*: Parker, J. R. (eds) *Petroleum Geology of Northwest Europe: Proceedings of the 4th Conference*. Geological Society, London, 1159–1166.

FÆRSETH, R. B. 1996. Interaction of Permo-Triassic and Jurassic extensional fault-blocks during the development of the northern North Sea. *Journal of the Geological Society, London*, 153, 931–944.

FOWLER, S. & McKENZIE, D. P. 1989. Gravity studies of the Rockall and Exmouth Plateaux using SEASAT altimetry. *Basin Research*, 2, 27–34.

GILTNER, J. P. 1987. Application of extensional models to the Northern Viking Graben. *Norsk Geologisk Tidsskrift*, 67, 339–352.

HAQ, B., HARDENBOL, J. & VAIL, P. R. 1987. Chronology of fluctuating sea level since the Triassic (250 million years to present). *Science*, 25, 1156–1167.

HAYWARD, N. J. & EBINGER, C. J. 1996. Variations in the along strike segmentation of the Afar rift system. *Tectonics*, 15, 244–257.

HENDRIE, D. B., KUSZNIR, N. J. & HUNTER, R. H. 1993. Jurassic extension estimates for the North Sea 'triple junction' from flexural backstripping: implications for decompression melting models. *Earth and Planetary Science Letters*, 116, 113–127.

HOLLANDER, N. B. 1987. Snorre. *In*: Spencer, A. M. *et al.* (eds) *Geology of the Norwegian Oil and Gas Fields*. Graham & Trotman, London, 307–318.

HOLLIGER, K. & KLEMPERER, S. L. 1990. Gravity and deep seismic reflection profiles across the North Sea rifts. *In*: Blundell, D. J. & Gibbs, A. D. (eds) *Tectonic Evolution of the North Sea Rifts*. Oxford University Press, Oxford, 82–100.

JACKSON, J. A. 1987. Active normal faulting and crustal extension. *In*: Coward, M. P., Dewey, J. F. & Hancock, P. L. (eds) *Continental Extensional Tectonics*. Geological Society, London, Special Publications, 28, 3–17.

JARVIS, G. T. & McKENZIE, D. P. 1980. Sedimentary basin formation with finite extension rates. *Earth and Planetary Science Letters*, 48, 42–52.

KUSZNIR, N. J., MARSDEN, G. & EGAN, S. S. 1991. A flexural cantilever simple-shear/pure-shear model of continental lithosphere extension: application to the Jeanne d'Arc Basin and Viking Graben. *In*: Roberts, A. M., Yielding, G. & Freeman, B. (eds) *The Geometry of Normal Faults*. Geological Society, London, Special Publications, 56, 41–60.

——, ROBERTS, A. M. & MORLEY, C. 1995. Forward and Reverse Modelling of Rift Basin Formation. *In*: Lambiase, J. (ed.) *Hydrocarbon Habitat in Rift Basins*. Geological Society, London, Special Publications, 80, 33–56.

LERVIK, K. S., SPENCER, A. M. & WARRINGTON, G. 1989. Outline of Triassic stratigraphy and structure in the central and northern North Sea. *In*: Collinson, J. D. (ed.) *Correlation in Hydrocarbon Exploration*, (Norwegian Petroleum Society) Graham & Trotman, London, 173–189.

LIVERA, S. E. & GDULA, J. E. 1990. Brent Oil Field. *In*: Beaumont, E. A. & Foster, N. H. (eds) *Atlas of Oil and Gas Fields, Structural Traps II, Traps Associated with Tectonic Faulting*. American Association of Petroleum Geologists, 21–63.

MAGNAVITA, L. P., DAVISON, I. & KUSZNIR, N. J. 1994. Rifting, erosion and uplift history of the Reconcavo–Tucano–Jatoba Rift, northern Brazil. *Tectonics*, 13, 367–388.

McKENZIE, D. P. 1978. Some remarks on the development of sedimentary basins. *Earth and Planetary Science Letters*, 40, 25–32.

—— & FAIRHEAD, D. 1997. Estimates of the effective elastic thickness of the continental lithosphere from Bouguer and free air gravity anomalies. *Journal of Geophysical Research*, 102, 27 523–27 552.

NADIN, P. A. & KUSZNIR, N. J. 1995. Palaeocene uplift and Eocene subsidence in the northern North Sea Basin from 2D forward and reverse stratigraphic modelling. *Journal of the Geological Society, London*, 152, 833–848.

—— & —— 1996. Forward and reverse stratigraphic modelling of Cretaceous-Tertiary post-rift subsidence and Palaeogene uplift in the Outer Moray Firth Basin, central North Sea. In: Knox, R. W. O'B., Corfield, R. M. & Dunay, R. E. (eds) *Correlation of the Early Palaeogene in Northwest Europe*. Geological Society, London, Special Publications, 101, 43–62.

NORRIS, S. & KUSZNIR, N. J. 1993. 3-D reverse modelling of post-rift extensional basins. *Terra Nova*, 5, 173–174.

PRICE, J. D., DYER, R., GOODALL, I., McKIE, T., WATSON, P. & WILLIAMS, G. 1993. Effective stratigraphical subdivision of the Humber Group and the Late Jurassic evolution of the UK Central Graben. *In*: Parker, J. R. (eds) *Petroleum Geology of Northwest Europe: Proceedings of the 4th Conference*. Geological Society, London, 443–458.

ROBERTS, A. M., LUNDIN, E. R. & KUSZNIR, N. J. 1997. Subsidence of the Vøring Basin and the influence of the Atlantic continental margin. *Journal of the Geological Society, London*, 154, 551–557.

——, PRICE, J. D. & OLSEN, T. S. 1990. Late Jurassic half-graben control on the siting and structure of hydrocarbon accumulations: UK/Norwegian Central Graben. *In*: Hardman, R. F. P. & Brooks, J. (eds) *Tectonic Events Responsible for Britain's Oil and Gas Reserves*. Geological Society, London, Special Publications, 55, 229–258.

——, YIELDING, G. & BADLEY, M. E. 1993*a*. Tectonic and bathymetric controls on stratigraphic sequences within evolving half-graben. *In*: Williams, G. D. & Dobb, A. (eds) *Tectonics and Seismic Sequence Stratigraphy*. Geological Society, London, Special Publication, 71, 87–121.

——, ——, KUSZNIR, N. J., WALKER, I. & DORN-LOPEZ, D. 1993*b*. Mesozoic extension in the North Sea: constraints from flexural backstripping, forward modelling and fault populations. *In*: Parker, J. R. (eds)

Petroleum Geology of Northwest Europe: Proceedings of the 4th Conference. The Geological Society, London, 1123–1136.

——, ——, ——, —— & —— 1995. Quantitative analysis of Triassic extension in the Northern Viking Graben. *Journal of the Geological Society, London*, 152, 15–26.

SCLATER, J. G. & CHRISTIE, P. A. F. 1980. Continental Stretching: an explanation of the post mid-Cretaceous subsidence of the Central North Sea Basin. *Journal of Geophysical Research*, 85, 3711–3739.

SØRENSEN, K. 1986. Danish Basin subsidence by Triassic rifting on a lithosphere cooling background. *Nature*, 319, 660–663.

SPENCER, A. M. & LARSEN, V. B. 1990. Fault traps in the Northern North Sea. *In*: Hardman, R. F. P. & Brooks, J. (eds) *Tectonic Events Responsible for Britain's Oil and Gas Reserves*. Geological Society, London, Special Publications, 55, 281–298.

STECKLER, M. S. & WATTS, A. B. 1978. Subsidence of the Atlantic-type continental margin off New York. *Earth and Planetary Science Letters*, 41, 1–13.

TURCOTTE, D. L. & SCHUBERT, G. 1982. *Geodynamics*. Wiley, Chichester.

WALKER, I. M., BERRY, K. A., BRUCE, J. R., BYSTØL, L. & SNOW, J. H. 1997. Structural modelling of regional depth profiles in the Vøring Basin: implications for the structural and stratigraphic development of the Norwegian passive margin. *Journal of the Geological Society, London*, 154, 537–544.

WATTS, A. B. & TORNÉ, M. 1992. Crustal structure and the mechanical properties of extended continental lithosphere in the Valencia trough (western Mediterranean). *Journal of the Geological Society, London*, 149, 813–827.

——, KARNER, G. D. & STECKLER, M. S. 1982. Lithospheric flexure and the evolution of sedimentary basins. *Philosophical Transactions of the Royal Society, London*, 305, 249–281.

WHITE, N. J. 1990. Does the uniform stretching model work in the North Sea? *In*: Blundell, D. J. & Gibbs, A. D. (eds) *Tectonic Evolution of the North Sea Rifts*. Oxford University Press, Oxford, 217–240.

—— & LATIN, D. M. 1993. Subsidence analyses from the North Sea 'triple junction'. *Journal of the Geological Society, London*, 150, 473–488.

YIELDING, G., BADLEY, M. E. & ROBERTS, A. M. 1992. The structural evolution of the Brent Province. *In*: Morton, A. C., Haszeldine, R. S., Giles, M. R. & Brown, S. (eds) *Geology of the Brent Group*. Geological Society, London, Special Publications, 61, 27–44.

Received 19 June 1997; revised typescript accepted 13 July 1998.